https://ntrs.nasa.gov/search.jsp?R=19790004052 2020-03-22T00:44:42+00:00Z


# General Disclaimer

## One or more of the Following Statements may affect this Document

- This document has been reproduced from the best copy furnished by the organizational source. It is being released in the interest of making available as much information as possible.

- This document may contain data, which exceeds the sheet parameters. It was furnished in this condition by the organizational source and is the best copy available.

- This document may contain tone-on-tone or color graphs, charts and/or pictures, which have been reproduced in black and white.

- This document is paginated as submitted by the original source.

- Portions of this document are not fully legible due to the historical nature of some of the material. However, it is the best reproduction available from the original submission.

Produced by the NASA Center for Aerospace Information (CASI)

NASA
Technical Memorandum 79022

AVRADCOM
Technical Report 78-52

(NASA-TM-79022) DEVELOPMENT OF SPRAYED CERAMIC SEAL SYSTEMS FOR TURBINE GAS PATH SEALING (NASA) 22 p HC A02/MF A01 CSCL 11A

N79-12223

Unclas
G3/27 38846

# DEVELOPMENT OF SPRAYED CERAMIC SEAL SYSTEM FOR TURBINE GAS PATH SEALING

Robert C. Bill
Propulsion Laboratory
AVRADCOM Research and Technology Laboratories
Lewis Research Center
Cleveland, Ohio

and

L. T. Shiembob and O. L. Stewart
Pratt & Whitney Aircraft Group
United Technologies Corporation
East Hartford, Connecticut

DEC 1978
RECEIVED
NASA STI FACILITY

TECHNICAL PAPER to be presented at the
Winter Annual Meeting
sponsored by the American Society of Mechanical Engineers
San Francisco, California, December 10-15, 1978

NASA
Technical Memorandum 79022

AVRADCOM
Technical Report 78-52

(NASA-TM-79022) DEVELOPMENT OF SPRAYED CERAMIC SEAL SYSTEMS FOR TURBINE GAS PATH SEALING (NASA) 22 p HC A02/MF A01 CSCL 11A

N79-12223

Unclas
G3/27 38846

# DEVELOPMENT OF SPRAYED CERAMIC SEAL SYSTEM FOR TURBINE GAS PATH SEALING

Robert C. Bill
Propulsion Laboratory
AVRADCOM Research and Technology Laboratories
Lewis Research Center
Cleveland, Ohio

and

L. T. Shiembob and O. L. Stewart
Pratt & Whitney Aircraft Group
United Technologies Corporation
East Hartford, Connecticut

DEC 1978
RECEIVED

TECHNICAL PAPER to be presented at the
Winter Annual Meeting
sponsored by the American Society of Mechanical Engineers
San Francisco, California, December 10-15, 1978

E-9819

# DEVELOPMENT OF SPRAYED CERAMIC SEAL SYSTEM FOR TURBINE GAS PATH SEALING

by R. C. Bill,* L. T. Shiembob,** and O. L. Stewart**

Lewis Research Center

## ABSTRACT

Analytical and experimental research was conducted to evaluate a ceramic seal system for a high pressure turbine employing plasma-sprayed graded metal/ceramic yttria stabilized zirconium oxide (YSZ). The performance characteristics of several YSZ configurations were determined through rig testing for thermal shock resistance, abradability, and erosion resistance. Results from this work indicate that this type of sealing system offers the potential to meet the operating requirements of future gas turbine engines. However, further development and refinement of this technology, particularly in the area of improving cyclic thermal stress tolerance, is necessary.

## INTRODUCTION

The efficiency of a gas turbine engine is sensitive to the operating clearance between the tips of the turbine blades and the stationary gas path seal components over the blade tips. Studies have indicate that in high reaction turbine designs, approximately 3 percent turbine efficiency loss is suffered for each 1 percent increase in blade tip clearance to blade span ratio (ref. 1). In a typical large commercial aircraft engine, this means that for each 0.010 in. increase in clearance over the high pressure turbine (HPT) blade tips, a 0.5 to 1.0 percent penalty in thrust specific fuel consumption (TSFC) results. Translated into fuel consumption, approximately $10^6$ bbl/yr additional fuel is consumed for each 0.010 in. increase in HPT tip clearance for the wide bodies jet fleet in this country alone.

Current state-of-the-art in turbine tip sealing technology is based on metallic material systems. Cast superalloy seal shroud segments, sintered or hot pressed

*AVRADCOM Research and Technology Laboratories.

**Pratt & Whitney Aircraft Group, United Technologies Corp.

powder metal seal shrouds, and thermal sprayed metallic systems are employed in various turbine seal applications. To cope with the high turbine gas temperatures, these metallic systems require substantial amounts of cooling air with an associated engine efficiency penalty. Furthermore, these materials are prone to gradual clearance degradation through erosive and corrosive mechanisms.

An attractive alternate turbine sealing approach, especially considering the overall trend of increased turbine inlet temperatures in gas turbine technology, is to employ ceramic materials. As a class, ceramics retain their mechanical properties to significantly higher temperatures than metals, and, especially in the case of oxide ceramics, are chemically stable with respect to the turbine operating environment. These considerations lead to improved turbine seal performance from the standpoints of both reduced cooling air requirements and the potential to maintain small turbine tip clearances.

In order for ceramics to survive turbine operating conditions, however, they must be able to withstand the thermal shock conditions imposed on them as the engine goes through its cycle of operation. Brittle as they are when compared to metals, care must be taken in the design of ceramic components to ensure that they are not subject to excessive tensile stresses. In addition to withstanding cyclic thermal stresses, the turbine seal must also provide a degree of rub tolerance or abradability, and it must resist erosion if minimum turbine tip clearances are to be maintained.

In this paper, a ceramic HPT sealing approach employing plasma-sprayed yttria stabilized zirconium oxide (YSZ) is evaluated. Selection of plasma-sprayed YSZ was based on three factors: (1) chemical and structural stability of the material at temperatures well above those permissible for metallic systems; (2) potential cost effectiveness of the plasma-spray process; and (3) successful experience with similar materials in combustor liner applications.

The main objective of the evaluation was to study and develop methods of controlling thermal stresses, thereby providing cyclic thermal shock resistance to the plasma-sprayed YSZ seal system. Cyclic thermal shock test results and analytical highlights are presented in this paper. Evaluation of the rub tolerance and erosion resistance for the plasma-sprayed $ZrO_2$ turbine seal was undertaken, and the results are presented and compared with the performance of some metallic turbine seal systems.

## MATERIALS

The turbine seal system under development in this program consisted of a plasma-sprayed yttria stabilized zirconium oxide (YSZ) layer adjacent to the gas path. The starting ceramic powder was 19 w/o $Y_2O_3$ YSZ, in a mixed, nonprealloyed condition. Beneath this fully ceramic layer are various numbers and arrangements of mixed CoCrAlY - YSZ plasma-sprayed cermet layers. The plasma sprayed layers are applied to a cast MAR M-509 substrate. A cross section of a typical configuration is shown in figure 1. Spraying was performed using a rotating carousel fixture shown in figure 2. Specimens were mounted on the carousel, surfaces to be coated facing inward. During deposition, the carousel was rotated at about 300 rpm.

The functions of the intermediate cermet layers are to mitigate thermal stresses due to the engine operating cycle by: (1) grading the thermal expansion and elastic properties of the seal system in a stepwise manner between those of the YSZ and the MAR M-509 substrate; and (2) providing a somewhat compliant or resilient buffer between the YSZ and the MAR M-509. Measured physical and mechanical properties for each layer composition (except the NiCrAl bond layer) are summarized in table I. Representative micrographs showing porosity distribution and distribution of constituents in each of these layers are shown in figure 3.

### Cyclic Thermal Shock Resistance

The durability of the sprayed $ZrO_2$/CoCrAlY seal system in an engine application will depend greatly on its capability to successfully survive the initial and subsequent thermal cycles corresponding to the engine operational conditions. This is the most difficult parameter to satisfy with a ceramic seal because of the relatively low strength (especially tensile strength) of ceramic materials and the large mismatch in thermal growth between ceramic and metallic materials. The graded, layered system was designed specifically to modify the layer difference in the thermal expansion between the metal substrate and ceramic. Thermal and mechanical properties of each of the individual layers in the graded $ZrO_2$/CoCrAlY structure and the metal substrate, as well as the geometry of the seal segment and residual stress state, affect stresses generated during thermal cycling.

Thermal fatigue characteristics were evaluated in a test rig which subjected the seal specimens to a simulated gas turbine engine cycle from idle to sea level takeoff (SLTO) and back to idle, according to the thermal cycle shown in figure 4.

The thermal fatigue test rig is shown in figure 5. The specimen was mounted in a water cooled copper fixture. A combination of oxygen-propane torches and cooling air jets were used to achieve the desired thermal cycles on the $ZrO_2$ and metal substrate surfaces. The torches were mechanically moved toward or away from the specimen at controlled rates to provide the required thermal cycle. Fixed cooling air jets were turned on or off or the flow was changed at predetermined intervals to meet the cycle requirements. The $ZrO_2$ and metal substrate surface temperatures were monitored continuously with an optical pyrometer and thermocouples, respectively, and recorded on a strip chart.

The results of the cyclic thermal shock rig tests are summarized in figure 6, where the number of cycles required to initiate visible "mudflat" type cracks are shown for three different design variations. Also shown are analytically predicted maximum principal stress to strength ratios for each variation. The variations, shown schematically in figure 7, represent developmental steps in the design of the plasma sprayed turbine seal configuration. The four layer system was the first design configuration. Development of property data for the materials comprising the four layers permitted analytical evaluation of thermal stresses in the seal system, pointing the way to an improved configuration, the three layer system, and an experimental thermally prestressed system. Variations in configuration and prestress levels were thus analytically screened and selected with the aid of a specially adapted finite element stress analysis program described in more detail in reference 2.

Qualitative agreement between the analytical results and the experimental results summarized in figure 6 is observed to the extent that increased predicted stress-to-strength ratios in the ceramic layer correlate with reduced number of cycles to the first appearance of mudflat cracks.

With the exception of the thermal prestressed specimens, all of the thermal shock specimens survived a prescribed number of thermal cycles (100 for the four layer system, 500 for the three layer system) without loss of material through spallation. By the end of the test exposures however, laminar cracking in addition to mudflat cracking had occurred. The full extent of "mudflat" and laminar cracking is shown in figure 8 for the four layer system after 100 cycles and in figure 9 for the three layer system after 500 cycles. Laminar cracks result from both edge initiation, and the turning of propagating mudflat cracks (ref. 2).

The thermal prestressed specimen was prepared by spraying the cermet and zirconium oxide layers onto a preheated MAR M-509 substrate, maintained at about 1200$^{\circ}$ F during the spray process. Analysis, using previously obtained material properties, predicted the development of generally compressive stresses in the ceramic layer. It was expected that these compressive stresses would help prevent crack initiation. However, material properties gathered from thermally prestressed specimens, combined with actual thermal strain measurements, resulted in predicted failures near the ends of the seal specimens during the acceleration portion of the thermal cycle. In fact the mode of failure closely coincided in time and location with the analytically predicted failure. Adjustments to the thermal spray parameters combined with better controlled thermal prestress techniques are necessary for realization of the potential benefits of thermally prestressing the seal system.

Presently there is no clear way to predict cyclic life to spallation for the plasma-sprayed turbine seal systems. Obviously, the appearance of the first cracks in the ceramic layer is accompanied by considerable relief in thermal stresses. Experimental evidence exists (ref. 3), suggesting that growth of the mudflat and laminar cracks attenuates quite rapidly after their initial appearance. The prognosis for long cyclic thermal stress lives, with acceptable residual mechanical integrity, is considered good.

It is anticipated that improved cyclic thermal stress performance can be realized through better controlled thermal prestressing, and modifications to the microstructure of the ceramic layer. Increased porosity, modifications to pore size, shape, and distribution, and incorporation of fine, nonstabilized particles are modifications to the ceramic microstructure that have a chance of being realized in the plasma-sprayed process, and have shown promising thermal shock performance improvements (refs. 4, 5, and 6).

## Abradability

Abradability tests were performed on the test rig shown in figure 10. Twelve simulated turbine blade-tips made of B-1900 alloy (Ni-8 percent Cr-10 percent Co-1 percent Ti-6 percent Al-0.11 percent C) were mounted in the periphery of a disk. An air turbine was used to drive the disk so that the blade tip speed was 310 m/sec (1000 ft/sec). The seal segment specimen was mounted in a fixture at the end of a horizontal post attached to a movable carriage assembly. The carriage assembly injects the specimen radially into the rotor assembly at the required incursion rate. The seal specimen was heated from both sides of the rotor by oxygen-acetylene torches directed at the seal surface. Heating torches were also mounted off the carriage assembly. Firing rate and distance between the torches and seal specimen was varied to control the seal surface temperature, nominally 1309° C (2400° F) for all tests.

Seal surface temperature and blade tip temperature were monitored by optical pyrometers. Carriage travel was monitored by a linear differential transformer. A load cell in the carriage feed system permitted determination of the average normal force between the seal specimen and blade tips. All data were recorded continuously on a strip chart.

Blade tip and seal wear was determined through pre and post test measurements. Relative abradability between different specimens and different seal systems was assessed on the basis of the volume wear ratio (VWR) defined as the blade tip wear volume divided by the seal wear volume. The smaller the volume wear ratio, the better the abradability of the seal system.

The results of the abradability testing are shown in figure 11, where VWR is plotted as a function of incursion rate. Minimum VWR was measured under intermediate incursion rate conditions of $25.4\times10^{-6}$ m/sec ($1\times10^{-3}$ in./sec). A similar trend of minimum VWR under intermediate incursion rate conditions was observed in experiments performed on low density sintered NiCrAlY (ref. 7). It was proposed that for the sintered NiCrAlY, thermal effects promoted bulk softening and smearing of the low density seal material and consequent wear to the rotor under low incursion rate conditions. Metallographic sections, figure 12, show that even with plasma-sprayed zirconium oxide, a brittle ceramic material, rub induced smearing and surface densification do occur. Therefore the mechanism that promoted high wear to the rotor when rubbed against sintered NiCrAlY under low incursion rate conditions very likely promotes high rotor wear for the case of plasma-sprayed zirconium oxide. Heavy mechanical loading of the blade tips is believed to account for the increased blade tip wear under high incursion rates of $254\times10^{-6}$ m/sec (0.010 in./sec).

The condition of the seal specimen rub surface and distress to the blade tips resulting from a rub interaction at $25.4\times10^{-6}$ m/sec (1 in./sec) incursion rate are shown in figure 13. Particularly noteworthy are the smooth, glazed metal transfer film on the rub seal specimen rub surface, cracking in the transfer film (observed to propagate well into the ceramic), and the buildup of a back transferred metal prow on the leading edges of the blade tips.

The abradability of the plasma-sprayed zirconium oxide compares favorably with that of cast alloy shrouds currently used in high pressure turbine positions. It would be desirable to extend the envelope of favorable VWR over a broader range of parameters, particularly incursion rate. Hopefully, the provision of hard abrasive tip treatment being developed for high pressure turbine blades will provide improved abradability. Another approach to be considered in improving abradability is to reduce the ceramic layer density. This is not necessarily inconsistent with improving other aspects of seal performance such as thermal shock resistance (ref. 5).

## Erosion Resistance

Erosion tests were performed in the hot particulate erosion rig shown in figure 14. The specimen was positioned at the specified distance and impingement angle relative to the end of the combustor exit nozzle by a compound vise. The specimen was heated by impinging JP fuel and air combustion products on the $ZrO_2$ surface of the specimen through a 1.905 cm (0.75 in.) diameter exit nozzle. Specimen temperature and exit gas velocity were controlled by varying fuel and air flows. In all tests, the exit gas velocity was Mach 0.35, and the nozzle to specimen distance was 3.81 cm.

After the specimen temperature and gas velocity were stabilized, particulate flow was initiated. The particulate matter was gravity fed into a tube connected into the combustor exit nozzle approximately 5.08 cm (2 in.) upstream of the nozzle end where it was picked up and accelerated to the specimen surface by the hot gas stream. Particulate flow rate was controlled by a precalibrated orifice in the storage hopper discharge line. The weight of particulate used and the duration of particulate flow during the test was monitored to check the particulate flow rate. In all cases, the particulate material was 80 grit $Al_2O_3$, and the feed rate was 2.72 kg/hr (6.0 lb/hr).

Erosion tests were conducted at two specimen temperature levels: 1589 K ($2400^\circ$ F), and 1367 K ($2000^\circ$ F). Specimen temperature was measured optically on the $ZrO_2$ and metal substrate surfaces. Erosion wear was determined by measuring the weight loss of the specimen at 5 minute intervals.

Results are summarized in figure 15. Data presented in figure 15 indicate that both surface temperature and impingement angle have a significant effect upon erosion rate. The specimen tested at 1366 K ($2000^\circ$ F) and $15^\circ$ impingement angle exhibited an erosion rate approximately six times greater than specimens tested at 1589 K

(2400° F) at the same impingement angle. The specimen tested at 1589 K (2400° F) and 90° impingement angle exhibited an erosion rate approximately 20 times greater than specimens tested at the same temperature and 15° impingement angle.

A simplification of Bitter's equation (ref. 8), given below, was used to investigate erosion results.

$$Q = \frac{1/2\, M(V \sin \alpha - K)^2}{\epsilon}$$

where

Q wear due to repeated deformation, $cm^3$

M total mass of impinging particles, $gf\text{-}sec^2/cm$

V particle velocity before collision, cm/sec

K constant related to target properties, cm/sec

$\alpha$ impingement angle

$\epsilon$ deformation wear factor, $J/m^3$

For simplification K was assumed to be negligible in comparison to particle velocity - an assumption substantiated in the literature, reference 9. With this assumption the equation correlates well with the 1589 K (2400° F) data as shown in figure 15. The quantity $MV^2/2$ was evaluated at the 90° point by equating it to the measured erosion rate. Also the range of other high temperature seal systems such as sintered NiCoCrAlY and plasma sprayed CoCrAlY is indicated. The cause of the large scatter in the 1589 K (2400° F) data at 15° is not known but there are several possible explanations. They are: (1) batch to batch reproducibility of the sprayed $ZrO_2$ structure, (2) weight loss measurement error due to partial delamination of the coating during testing, or (3) a tendency toward ductile behavior. One or both of the first two are considered most likely since three out of four data points correlate very closely.

Generally speaking, the erosion resistance of the sprayed $ZrO_2$/CoCrAlY seal system appears to be marginally satisfactory for engine application. Some improvements is desirable if it can be obtained without much sacrifice in abradability or thermal fatigue resistance.

## CONCLUSIONS

Based on the analytical and experimental work described in this paper, the following conclusions regarding the plasma-sprayed YSZ high pressure turbine seal system are drawn:

(1) The most challenging aspect of performance of the seal system is the development of resistance to cyclic thermal stresses.

(2) Significant improvement in cyclic thermal stress resistance was realized through analytical optimization of the plasma-sprayed layer arrangements and thicknesses. Potential approaches to realizing further improvements were noted.

(3) Abradability of the plasma-sprayed YSZ layer is at least comparable to abradability of currently used HPT seal materials.

(4) Hot particulate erosion resistance of the plasma sprayed YSZ layer at its expected operating temperature compares favorably with metallic systems at their operating temperatures.

(5) Employing plasma-sprayed $ZrO_2$, in combination with some means of thermal stress mitigation, is considered an attractive approach to HPT sealing, and shows promise in terms of maintaining minimum clearances over the turbine blade tips.

## REFERENCES

1. Roelke, R. J., "Miscellaneous Losses - Tip Clearance and Disk Friction," Turbine Design and Application, Vol. 2, A. J. Glassman, ed., NASA SP-290, 1973, p. 125-148.
2. Shiembob, L. T., "Development of a Plasma Sprayed Ceramic Gas Path Seal for High Pressure Turbine Application," NASA CR-135183, 1977.
3. Shiembob, L. T., "Development of a Plasma Sprayed Ceramic Gas Path Seal for High Pressure Turbine Application," NASA CR-135387, May 1978.
4. Bill, R. C., and Wisander, D. W., "Preliminary Study of Cyclic Thermal Shock Resistance of Plasma Sprayed Zirconium Oxide Turbine Outer Air Seal Shrouds," NASA TM-73852, 1977.

5. Hasselman, D. P. H., "Unified Theory of Thermal Shock Fracture Initiation and Crack Propagation in Brittle Ceramics," Journal of the American Ceramic Society, Vol. 52, No. 11, Nov. 1969, pp. 600-604.

6. Claussen, N., "Stress-Induced Transformation of Tetragonal $ZrO_2$ Particles in Ceramic Matrices," Journal of American Ceramic Society, Vol. 61, No. 1-2, Jan.-Feb. 1978, pp. 85-86.

7. Bill, R. C., and Shiembob, L. T., "Friction and Wear of Sintered Fibermetal Abradable Seal Materials," NASA TM X-73650, 1977.

8. Bitter, J. G. A., "A Study of Erosion Phenomena, Part I," Wear, Vol. 6, 1963, pp. 5-21.

9. Neilson, J. H., and Gilchrist, A., "Erosion by a Stream of Solid Particles," Wear, Vol. 11, 1968, pp. 111-122.

TABLE I. - AVERAGE MODULI OF RUPTURE AND ELASTICITY AND STRAIN TO FAILURE TEST RESULTS

| Material | Test temperature | | Modulus of rupture | | Modulus of elasticity | | Strain to failure, percent |
|---|---|---|---|---|---|---|---|
| | K | $^{o}F$ | $10^3$ N/cm$^2$ | ($10^3$ psi) | $10^3$ N/cm$^2$ | ($10^6$ psi) | |
| 40/60 $ZrO_2$/CoCrAlY | 293 | (68) | 22.27 | (32.3) | 5.86 | (8.5) | 0.82 |
| | 1005 | (1350) | 10.83 | (15.7) | 9.24 | (13.4) | .39 |
| 70/30 $ZrO_2$/CoCrAlY | 293 | (68) | 5.63 | (8.16) | 3.62 | (5.25) | .43 |
| | 1061 | (1450) | 7.03 | (10.2) | 4.70 | (6.81) | .47 |
| 85/15 $ZrO_2$/CoCrAlY | 293 | (68) | 4.14 | (6.0) | 2.54 | (3.68) | .40 |
| | 1144 | (1600) | 4.70 | (6.82) | 1.86 | (2.70) | .34 |
| $ZrO_2$ | 293 | (68) | 2.82 | (4.09) | 4.69 | (6.8) | .12 |
| | 1589 | (2400) | 2.24 | (3.32) | 1.56 | (2.26) | .33 |

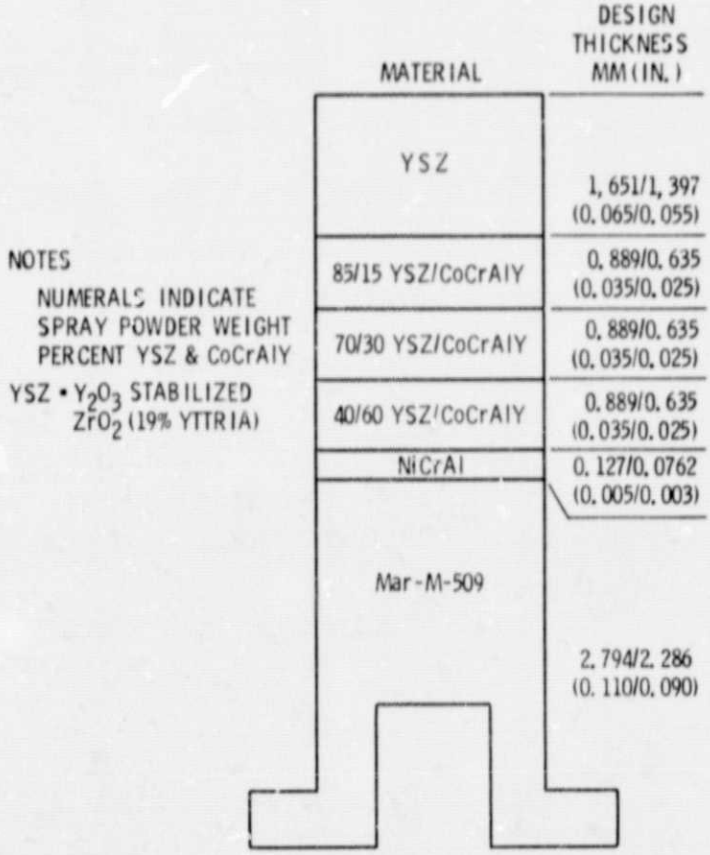


Figure 1. - Plasma sprayed graded layered $Y_2O_3$ stabilized $ZrO_2$/CoCrAlY seal system.

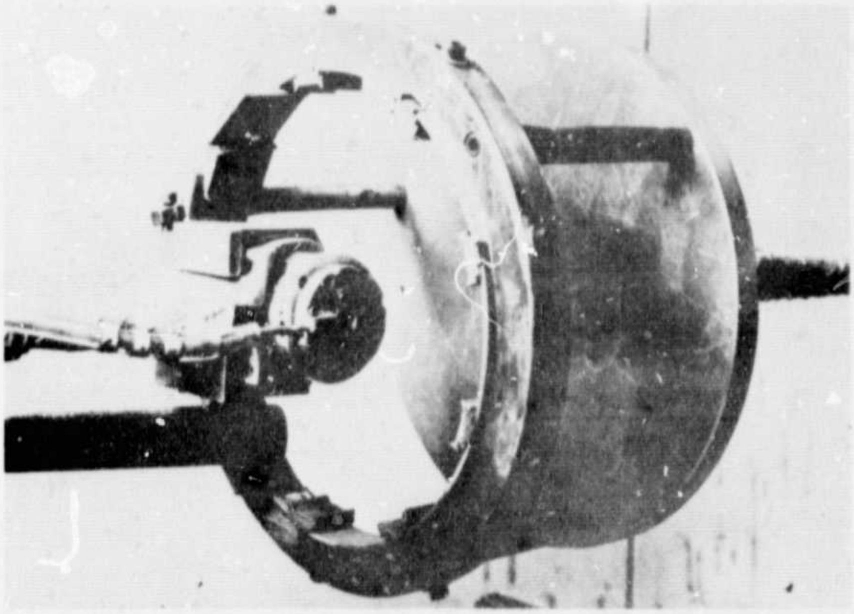

Figure 2. - Spray specimen fixture.

ORIGINAL PAGE IS
OF POOR QUALITY

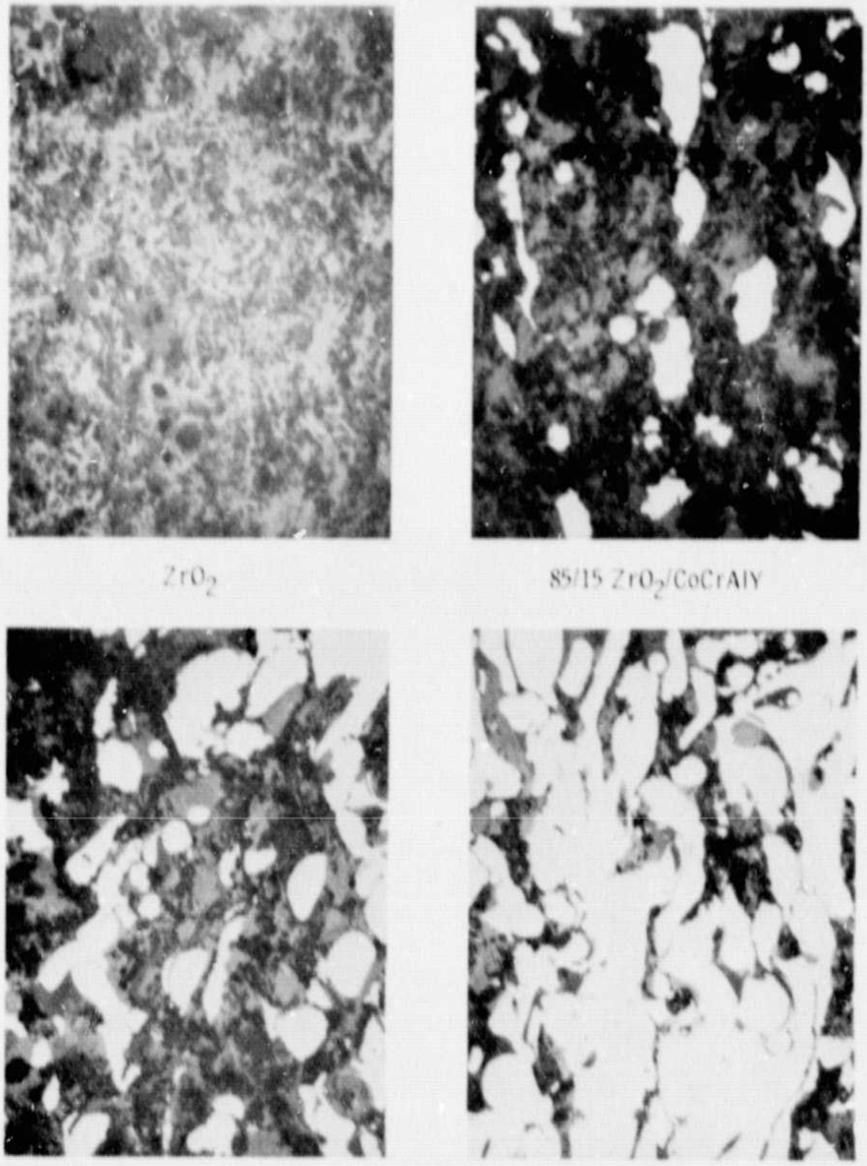

$ZrO_2$ | 85/15 $ZrO_2$/CoCrAlY

70/30 $ZrO_2$/CoCrAlY | 40/60 $ZrO_2$/CoCrAlY

Figure 3. - Microstructure of layers comprising the plasma sprayed seal system; X500, 37 percent reduction.

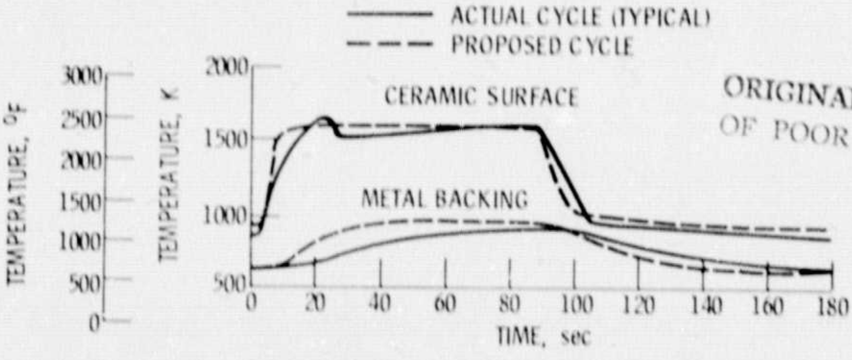


ORIGINAL PAGE IS
OF POOR QUALITY

Figure 4. - Thermal fatigue test cycle, abradability specimen.

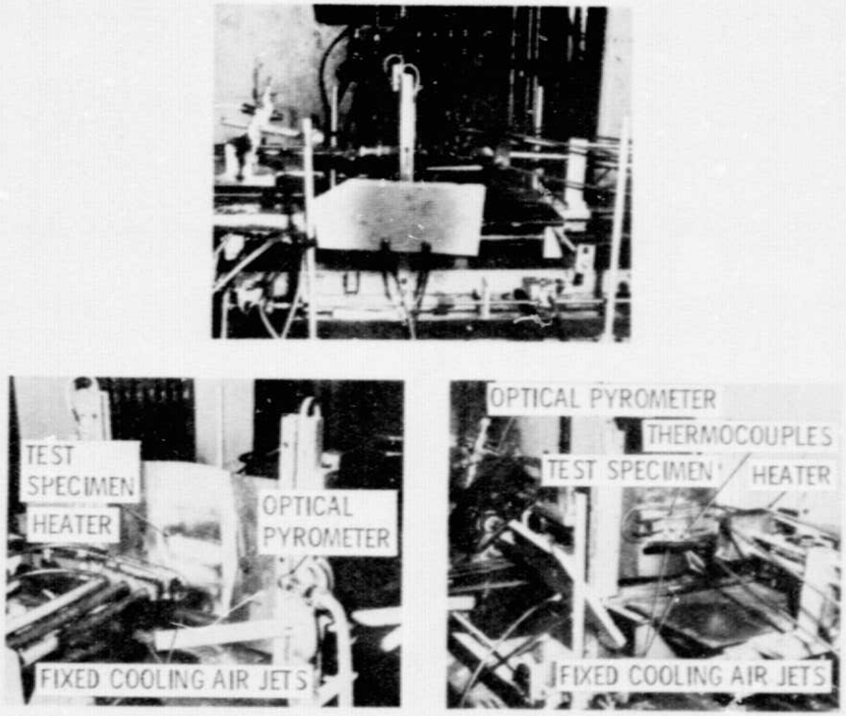


Figure 5. - Thermal shock rig.

ORIGINAL PAGE IS
OF POOR QUALITY

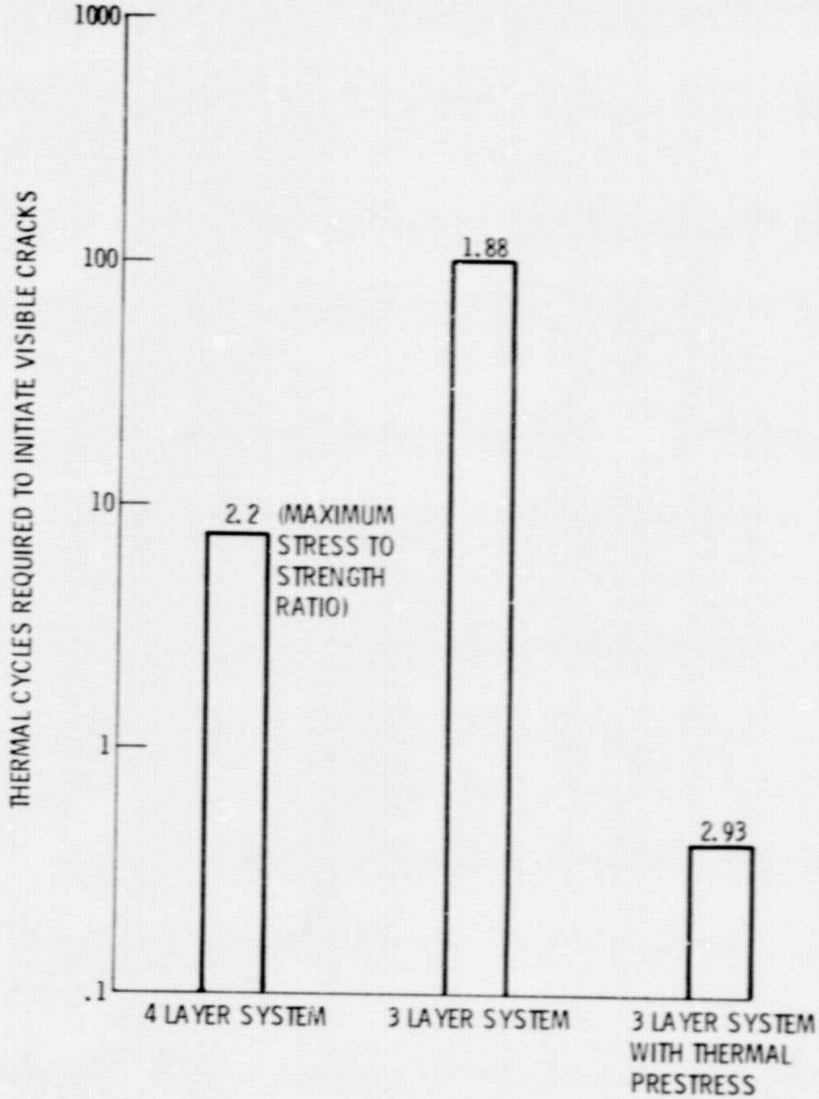


Figure 6. - Thermal shock cycles required to produce a visible crack network on the seal ceramic surface, for 3 seal design variations.

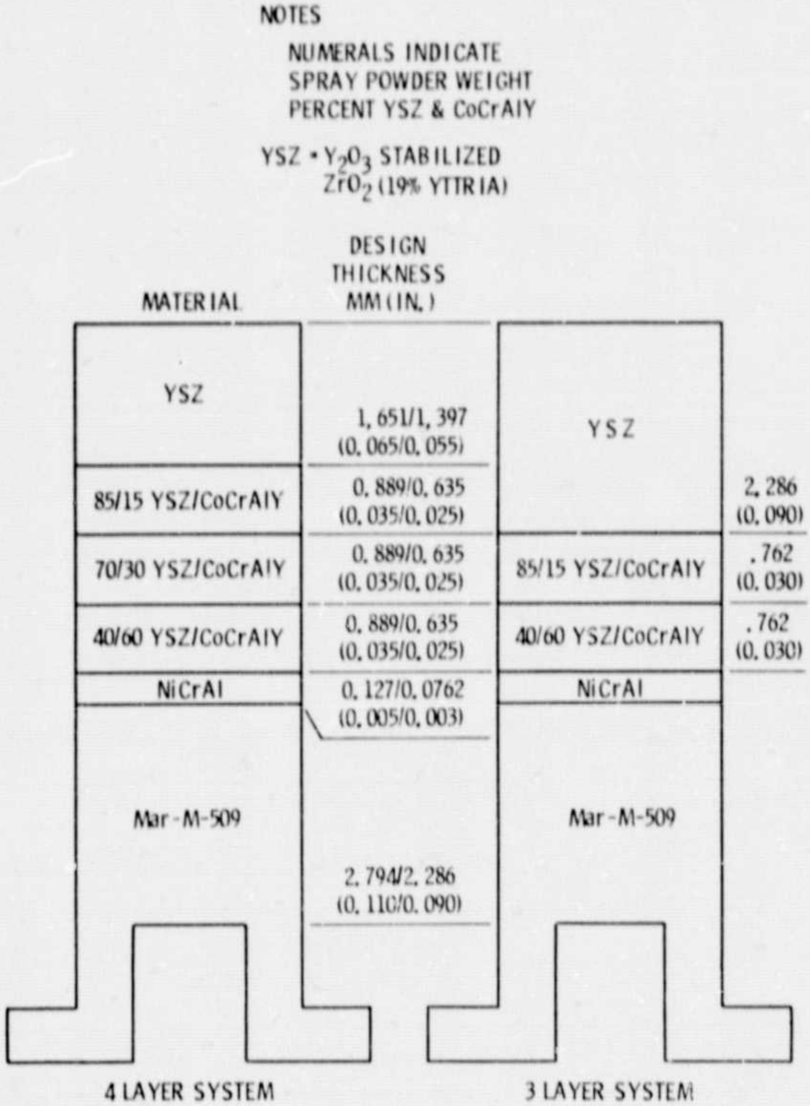


Figure 7. - Two design configuration variations of the plasma-sprayed ceramic turbine seal system.

ORIGINAL PAGE IS
OF POOR QUALITY

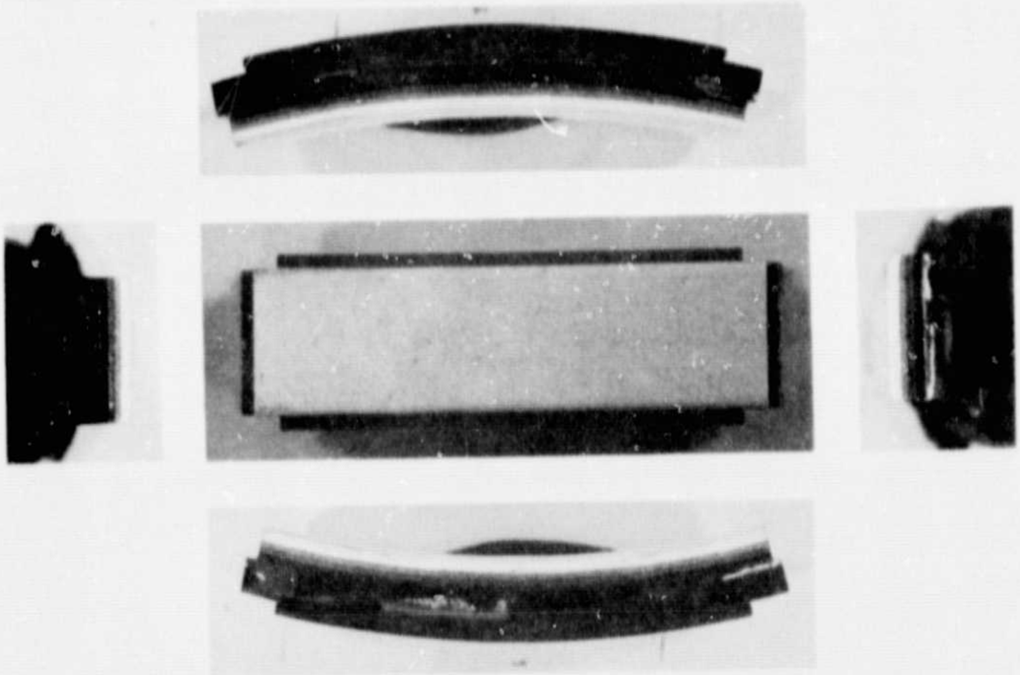

Figure 8. - Thermal fatigue specimen.

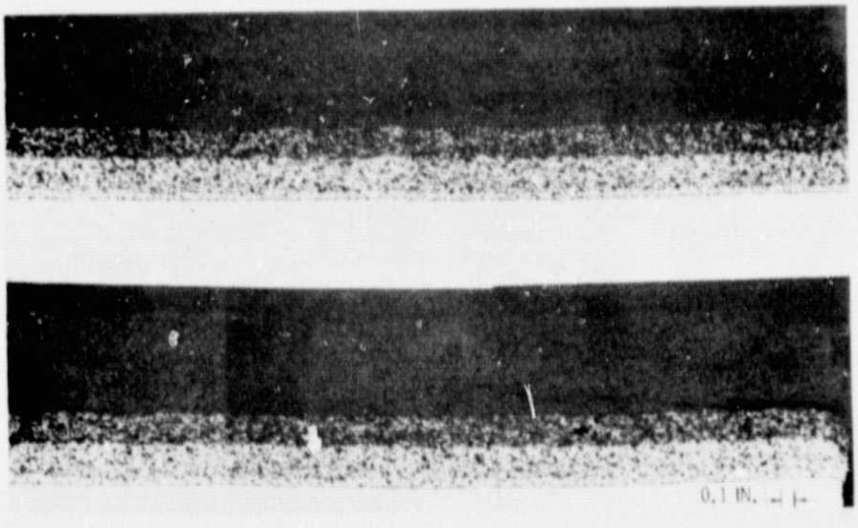


Figure 9. - Circumferential section through thermal fatigue specimen after 500 thermal shock cycles.

ORIGINAL PAGE IS
OF POOR QUALITY

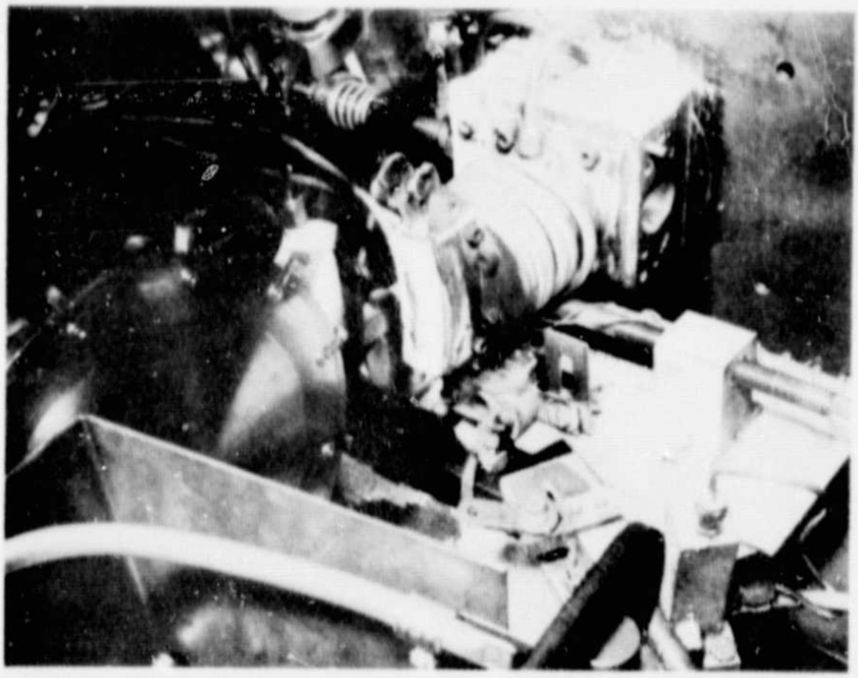

Figure 10. - High temperature abradability test rig. Note: Near side heating torch not shown.

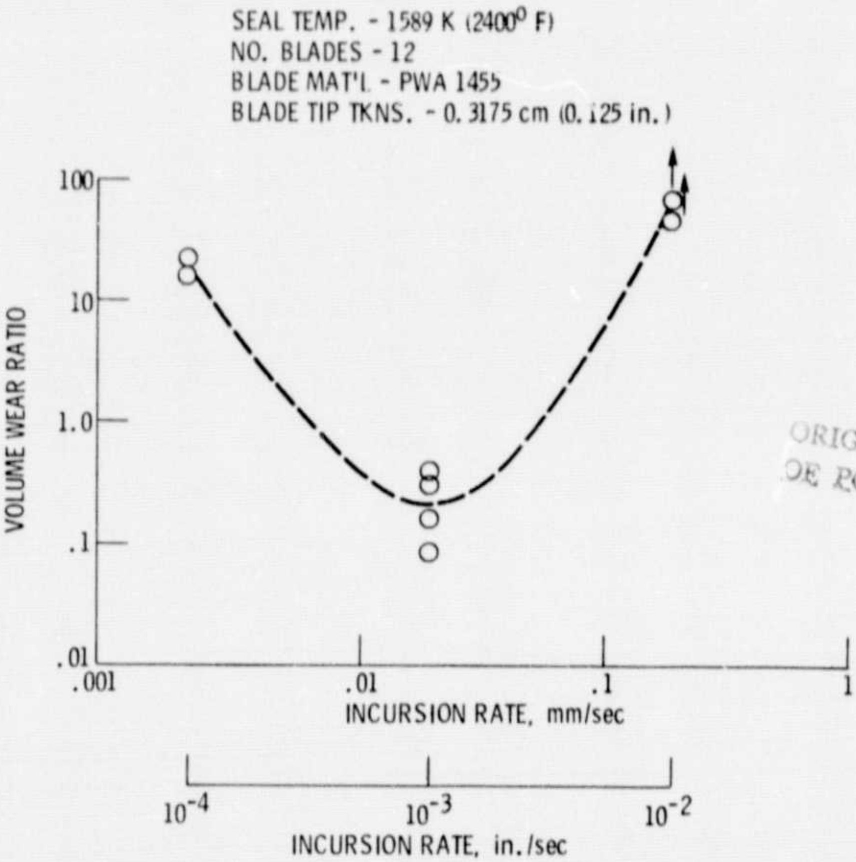


Figure 11. - Volume wear ratio as a function of incursion rate.

ORIGINAL PAGE IS
OF POOR QUALITY

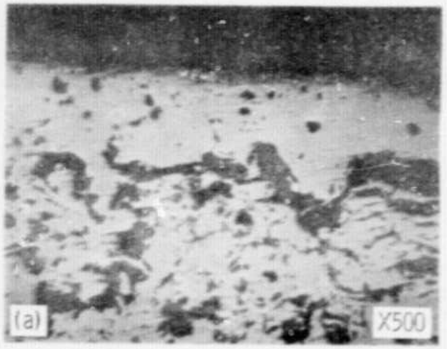


DESENSIFICATION OBSERVED AT SURFACE OF RUB PATH .002-.004 IN.

DEPOSIT (TRANSFER) REMNANTS ALSO OBSERVED AT SURFACE APPROX. .00024 IN. THICK

RUB DIRECTION →

OBSERVATION DIRECTION →

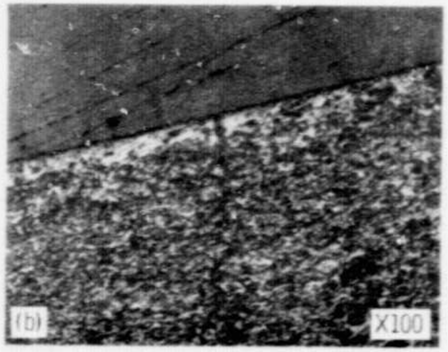


DESENISIFICATION OBSERVED ALONG LENGTH OF RUB PATH

CRACK ORIGIN APPEARS TO BE AT SURFACE

RUB DIRECTION →

OBSERVATION DIRECTION ↑

Figure 12. - Metal transfer and seal desensification in rub path.

ORIGINAL PAGE IS
OF POOR QUALITY

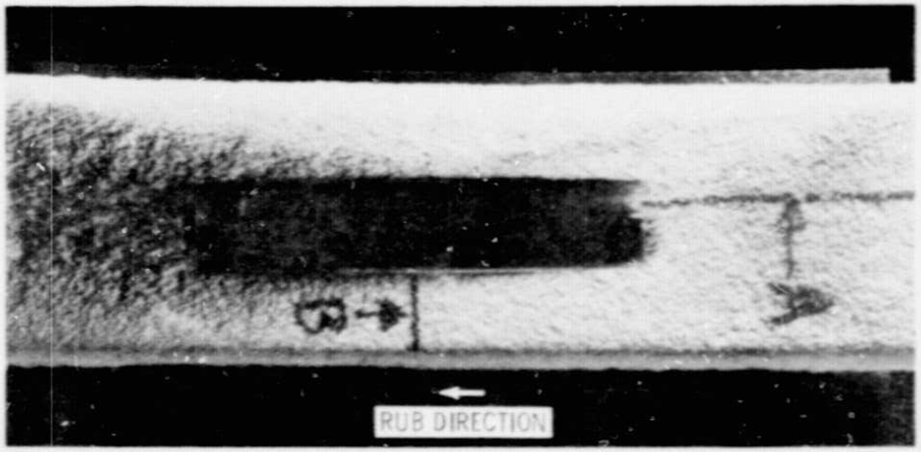


DIRECTION OF TRAVEL →

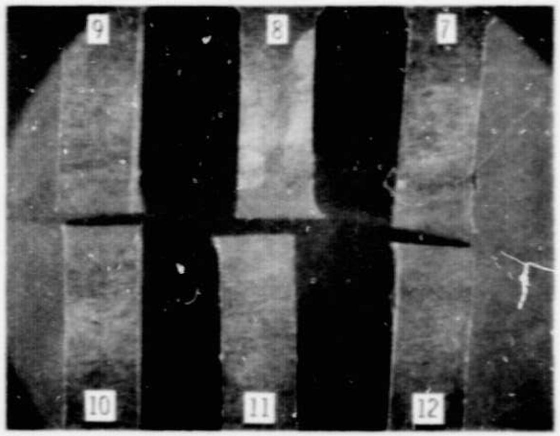


← DIRECTION OF TRAVEL

METAL PICKUP ON LEADING SIDE OF BLADES

Figure 13. - Seal specimen rub surface and blade tip condition after 1 mil/sec interaction at 2400° F.

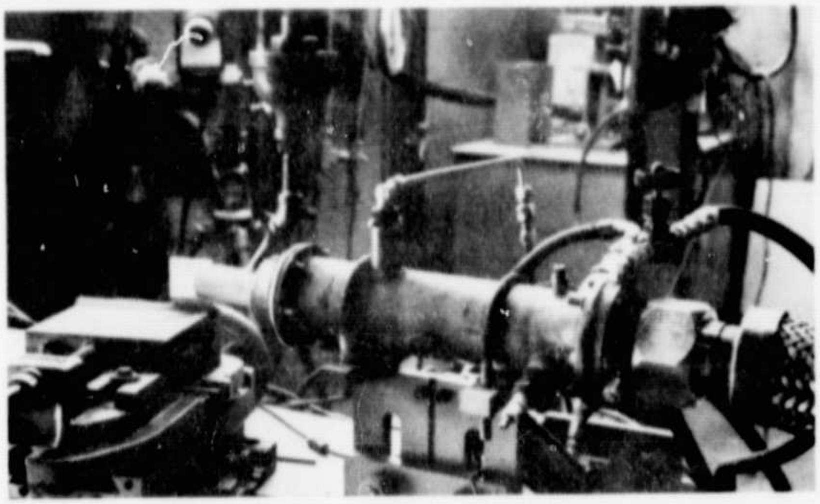

Figure 14. - Hot particulate erosion rig.

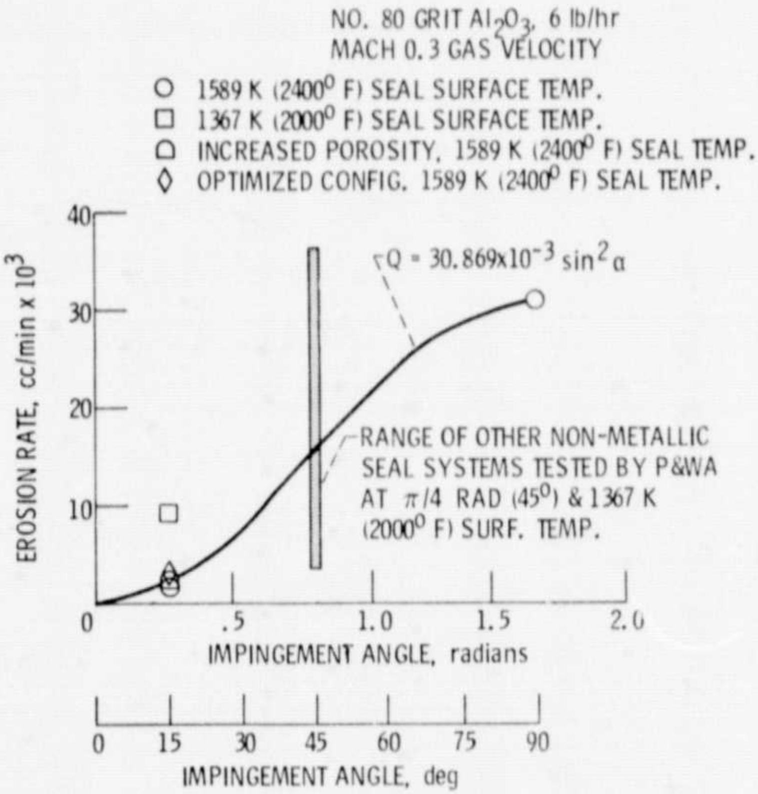


Figure 15. - Erosion test data correlation.

ORIGINAL PAGE IS
OF POOR QUALITY